



Aalborg Universitet

AALBORG UNIVERSITY  
DENMARK

## The Impact of Topology and Mission Profile on the Reliability of Boost-type Converters in PV Applications

Peyghami, Saeed; Davari, Pooya; Wang, Huai; Blaabjerg, Frede

*Published in:*

Proceedings of the 19th IEEE Workshop on Control and Modeling for Power Electronics (COMPEL)

*DOI (link to publication from Publisher):*

[10.1109/COMPEL.2018.8460177](https://doi.org/10.1109/COMPEL.2018.8460177)

*Publication date:*

2018

*Document Version*

Accepted author manuscript, peer reviewed version

[Link to publication from Aalborg University](#)

*Citation for published version (APA):*

Peyghami, S., Davari, P., Wang, H., & Blaabjerg, F. (2018). The Impact of Topology and Mission Profile on the Reliability of Boost-type Converters in PV Applications. In *Proceedings of the 19th IEEE Workshop on Control and Modeling for Power Electronics (COMPEL)* (pp. 1-8). [8460177] IEEE Press. IEEE Workshop on Control and Modeling for Power Electronics (COMPEL) <https://doi.org/10.1109/COMPEL.2018.8460177>

### General rights

Copyright and moral rights for the publications made accessible in the public portal are retained by the authors and/or other copyright owners and it is a condition of accessing publications that users recognise and abide by the legal requirements associated with these rights.

- Users may download and print one copy of any publication from the public portal for the purpose of private study or research.
- You may not further distribute the material or use it for any profit-making activity or commercial gain
- You may freely distribute the URL identifying the publication in the public portal -

### Take down policy

If you believe that this document breaches copyright please contact us at [vbn@aub.aau.dk](mailto:vbn@aub.aau.dk) providing details, and we will remove access to the work immediately and investigate your claim.

# The Impact of Topology and Mission Profile on the Reliability of Boost-type Converters in PV Applications

Saeed Peyghami, Pooya Davari, Huai Wang, and Frede Blaabjerg

*Department of Energy Technology*

*Aalborg University*

Aalborg, Denmark

sap@et.aau.dk, pda@et.aau.dk, hwa@et.aau.dk, fbl@et.aau.dk

**Abstract**—This paper investigates the impact of different converter topologies and mission profiles on the reliability of dc/dc boost-type PV converters. The reliability of three boost-type converters with the same input/output specifications is modeled employing a mission profile-based reliability evaluation method considering non-constant failure rate for the electrical components. This study identifies the contribution of active and passive components on the converter reliability for identifying the most failure prone components. Furthermore, the applicability of converter structures for different climate conditions is demonstrated seen from the reliability point of view.

**Keywords**— *reliability, mission profile, PV converter, boost converter, interleaved boost converter*

## I. INTRODUCTION

The global shift of energy paradigm towards carbon-free technologies has intensified the importance of power electronics technology in future power grids [1]–[3]. Power electronics play a main role in power conversion stage of energy resources, storages and loads. Meanwhile, dc grids are also becoming key enabling technologies [3], [4] for improving the power system reliability, availability and efficiency by integrating renewable energies like Photo Voltaic (PV) systems in order to support dc loads. Interfacing renewable resources with a fluctuating behavior may pose reliability challenges for power converters. This is due to the electro-mechanical stresses induced by power cycling, which may damage the active switches and capacitors that are the most fragile components of converters. Hence, reliability assessment of power converters especially in renewable applications is of significant importance.

Design for Reliability (DfR) is becoming more appealing especially for renewable applications [5], [6]. In this approach, power converter components are designed based on the target mission profile to approach a desired lifetime with an acceptable probability. The reliability of an

isolated dc/dc converter is analyzed for fuel-cell applications in [6]. The impact of mission profile on the reliability of IGBTs in a three-phase PV inverter is studied in [7], [8]. Other reliability evaluations of boost-based converters for PV applications have been presented in [9]–[12]. The main challenge of these studies is the assessment methodology based on reliability models presented in MIL-HDBK-217F [13] which do not take the temperature swing effect, as the most affecting parameter, into consideration. Furthermore, these studies assume a constant failure rate for different components based on [13]. Moreover, the introduced methodologies do not consider the effect of mission profiles on the reliability of power converters that can have a significant impact on the failure probability and different contributions of the electrical components on the overall reliability of the converter.

In this paper, a comprehensive reliability analysis of the dc/dc boost stage in PV applications is presented employing mission profile based modeling methods to investigate the impact of different topologies on the reliability of dc/dc boost stage in PV applications. The impact of climate conditions on the reliability of dc/dc PV converters and the applicability of converter topologies for different locations are analyzed. The main outcome is to provide a suitable insight in understanding the dependency of power electronic components and converter architecture on mission profile, in order to maximize the converter lifetime span in the application.

## II. PV CONVERTER STRUCTURES

In order to consider the effect of converter structure on the reliability of PV energy conversion system, three boost-based converters [9]–[12] including Single Boost (SB), Parallel Interleaved Boost (PIB) and Series Interleaved Boost (SIB) are considered as shown in Fig. 1. The capacity of each converter is 5 kW and the converters are designed to limit the input current ripple by 10% and the output voltage ripple by 0.5%. The specifications of the converters are summarized in Table I.

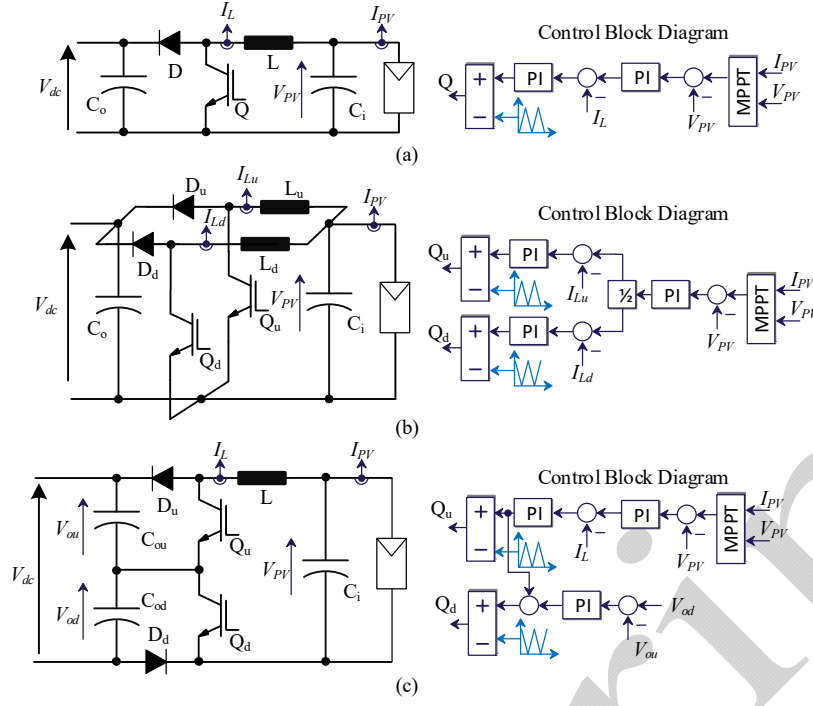


Fig. 1. Structure of dc/dc boost based converters for PV systems: (a) Single Boost (SB), (b) Parallel Interleaved Boost (PIB), (c) Series Interleaved Boost (SIB).

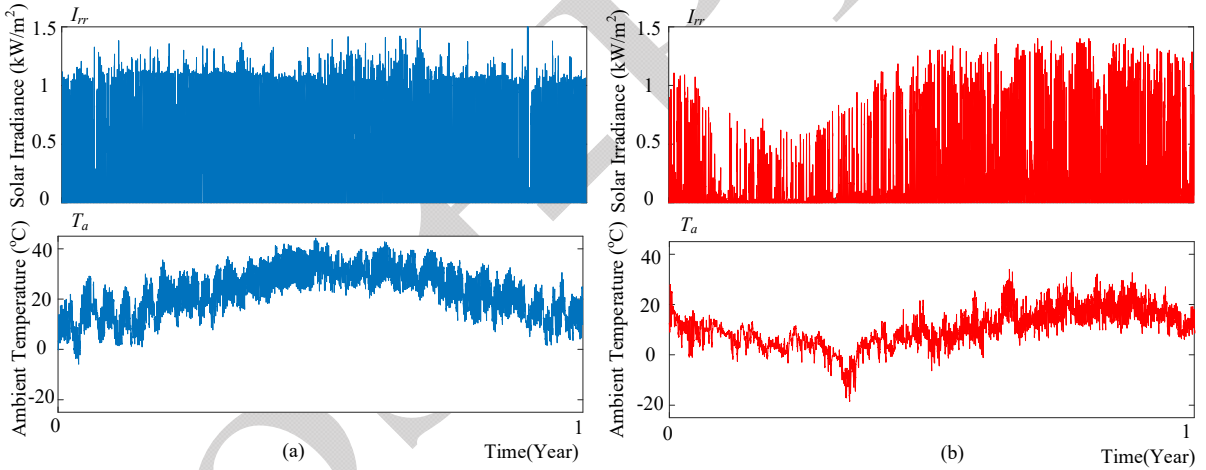


Fig. 2. Annual Solar Irradiance and ambient temperature in two different locations: (a) Location A, (b) Location B.

Table I. Specifications of dc/dc PV converters.

Topology	Capacity	Inductor (L)	Switching frequency	Output Voltage Ripple	Input Current Ripple	Diode (D) Switch (Q)	Capacitors ( $C_o$ ) EPCOS
SB	5 kW	2.2 mH	20 kHz	0.5% 1.8 V	10% 2 A	DV20E65D1 IGB10N60T	4×120 uF 450 V, 2.5 A
PIB	2×2.5 kW	2×1 mH	20 kHz	0.5% 1.8 V	10% 2 A	2×IDV15E65D2 2×IGP06N60T	2×120 uF 450 V, 2.5 A
SIB	5 kW	1 mH	10 kHz	0.5% 1.8 V	10% 2 A	2×DV20E65D1 2×IGB10N60T	2×(5×220 uF) 250 V, 2.2A

The studied PV system includes 3×8 PV panels of 210 W each with the parameters given in Table II. Furthermore, the PV system is modeled based on EN 50530:2010 [14] in order to fully consider the effect of solar Irradiance ( $I_{rr}$ ) and ambient temperature ( $T_a$ ). Fig. 2 shows the considered solar irradiance and ambient temperature data for two different locations. The illustrated annual solar irradiance ( $I_{rr}$ ) and

ambient temperature ( $T_a$ ) clearly show the difference in climate conditions of the two locations.

### III. POWER CONVERTER RELIABILITY ANALYSIS

It is well-known that active switches and capacitors are two of the fragile components in power converters. In order to estimate stresses or damages on the devices, one-year

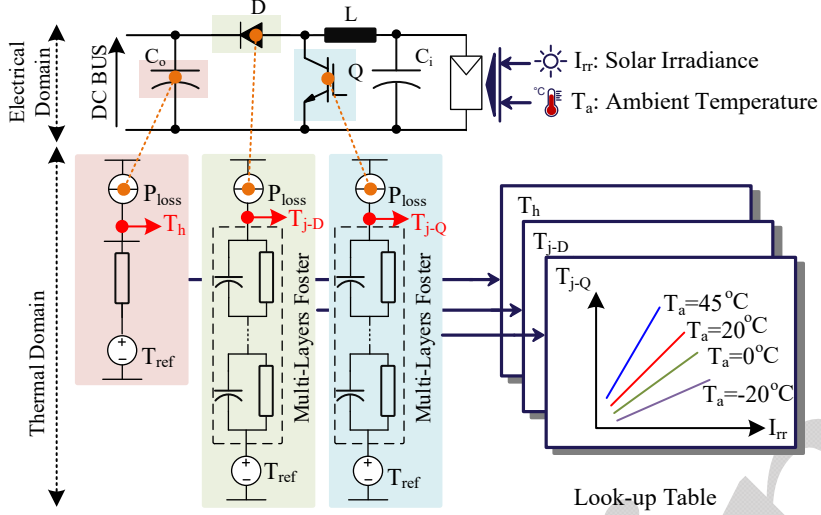


Fig. 3. Electro-thermal modelling of dc/dc boost converter in Fig. 1.

Table II. Specifications of PV Panels and PV System.

Parameter	Symbol	Value
Panel Rated Power	$P_r$ (W)	210
Open Circuit Voltage	$V_{oc}$ (V)	37.75
Short Circuit Current	$I_{sc}$ (A)	8
MPPT Voltage	$V_m$ (V)	32.3
MPPT Current	$I_m$ (A)	6.5
Voltage temp. Coeff.	$\alpha$ (%/K)	-0.34
Current temp. Coeff.	$\beta$ (%/K)	0.035
Number of Series panels	$N_s$	8
Number of Parallel panels	$N_p$	3

solar irradiance and ambient temperature profile for two different locations are considered. Thereafter, electro-thermal analyses have been performed to estimate the thermal stress on the devices induced by the irradiance and ambient temperature variations.

#### A. Thermal analysis

Thermal stresses on each component can be obtained by introducing an appropriate electro-thermal model, which translates the electrical stresses to the thermal stresses on the devices. The electro-thermal model of the output electrolytic capacitor, switch and diode of the SB is shown in Fig. 3. The thermal parameters are obtained from the datasheets and summarized in Table III. Effect of input capacitor ( $C_i$ ) can be neglected as the Boost inductor filters the high frequency currents. In order to model the thermal behavior of the converters, the temperature of the components is obtained by simulation with *PLECS* under different ambient temperatures and solar irradiances. The junction temperature of active switches and hot spot temperature of capacitors can then be calculated and stored in look-up tables.

#### B. Reliability calculation of electrolytic capacitors

Based on the state-of-the-art lifetime models for capacitors, the lifetime of electrolytic capacitors can be

Table III. Thermal Constants of active and passive components.

Component		ESR ( $\Omega$ )	Thermal resistance (K/W)	Thermal time constant (s)
Capacitor	120 uF 2.5 A	0.266	22	600
	220 uF 2.2 A	0.350	30	600
Diode	DV20E65D1	-	0.1317	28.14
			1.621	2.428
			0.8924	2.231
	IDV15E65D2	-	0.4108	0.0242
			0.1299	28.28
			1.58	2.43
IGBT	IGB10N60T	-	0.8892	0.3547
			0.472	0.0237
			0.2911	0.0653
	IGP06N60T	-	0.4092	0.00833
			0.5008	0.000737
			0.1529	0.000076
			0.3837	0.0504
			0.4533	0.0047
			0.5877	0.0004
			0.2483	0.0001

affected by the temperature and voltage stress as given in (1) [15]:

$$L_t = L_o \cdot 2^{\frac{T_o - T_t}{n_1}} \left( \frac{V_t}{V_o} \right)^{-n_2} \quad (1)$$

where  $L_o$  and  $L_t$  are the lifetime under rated and applied conditions,  $T_o$  and  $T_t$  are the rated and applied temperature, and  $V_o$  and  $V_t$  are the rated and applied voltage. Parameters  $n_1$  and  $n_2$  are the temperature dependent constant and voltage stress exponent [15]. Following [15], in this paper  $n_1 = 10$  and  $n_2 = -3$ . The thermal damage on the capacitors can be calculated based on the Minor rule as given in (2):

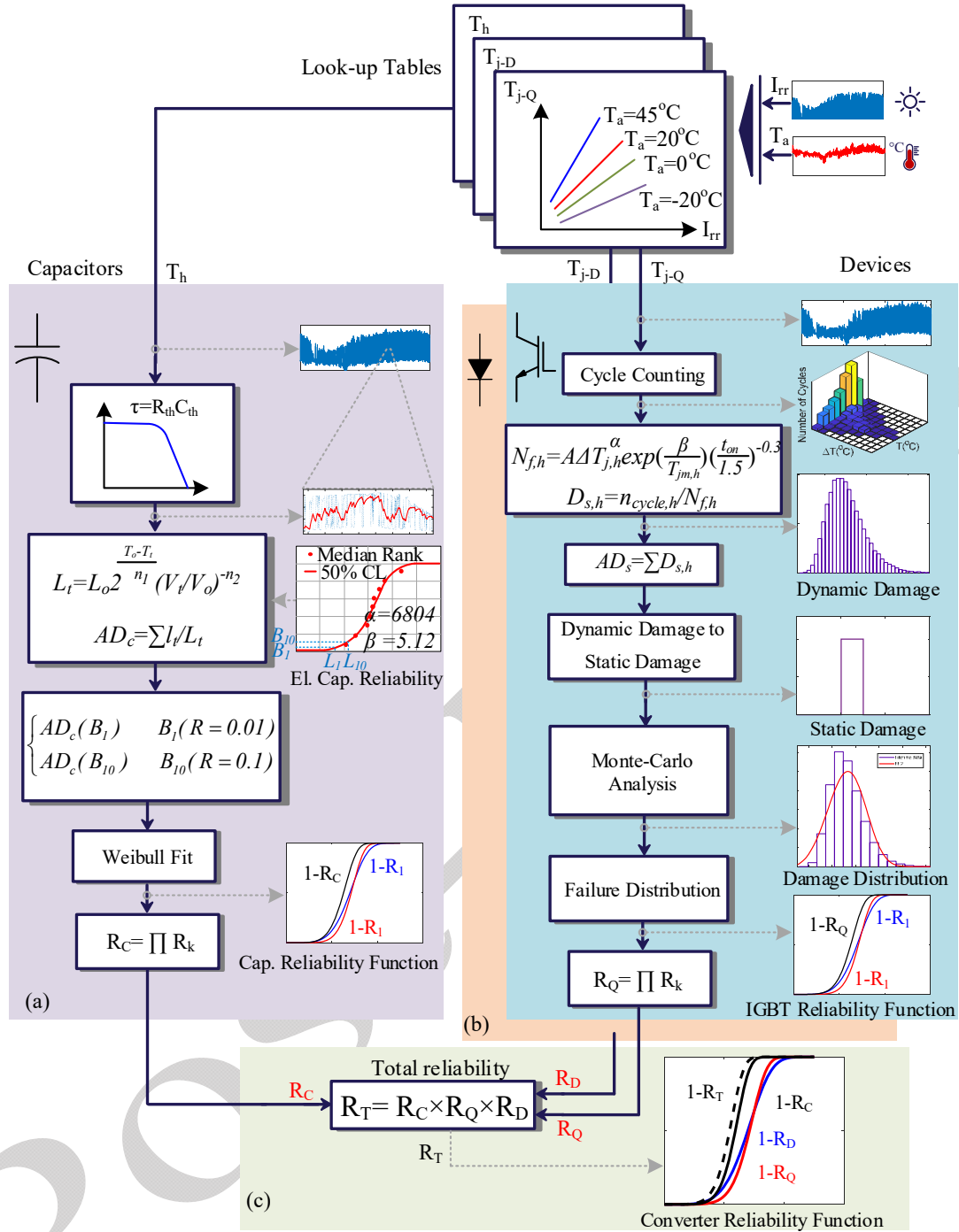


Fig. 4. Reliability estimation procedure of a power converter: (a) electrolytic capacitors, (b) active switches (Diode and IGBT).

$$AD_c = \sum \frac{l_t}{L_t} \quad (2)$$

where  $AD_c$  is the accumulated damage,  $L_t$  is the estimated lifetime based on (1), and  $l_t$  is the time interval the capacitor stays under temperature  $T_t$  and voltage  $V_t$ .  $l_t$  is equal to the consumed lifetime of capacitor under the mentioned stresses. The reciprocal of  $AD_c$  will give lifetime of the capacitor if the yearly mission profile is applied.

In order to find the failure probability function, the measured test data for a radial lead electrolytic capacitors with the rated lifetime of 5000 hours at the rated ripple

current and upper category temperature of 105 °C is used, where  $9 \times (56 \mu\text{F} / 35 \text{ V})$  electrolytic capacitors were tested [6]. The selected output capacitors for dc/dc converters belong to these type of capacitors. Hence, the  $B_1$ ,  $B_{10}$  damage and consequently  $B_1$ ,  $B_{10}$  lifetime of capacitors can be calculated based on the real test data [6]. The obtained lifetime data for  $B_1$ ,  $B_{10}$  can be used to find out the Weibull-based unreliability functions [6]. Finally, the total reliability of the output capacitor bank (i.e., series and parallel connection of the capacitors for enough current rating) can be found by using a series reliability network model. The procedure of capacitor lifetime estimation is

shown in Fig. 4 (a). Notably, the thermal time constant of electrolytic capacitors are relatively high. In order to consider the effect of thermal capacitance ( $C_{th}$ ) on the hot spot temperature of capacitors, the temperature data are passed through a low pass filter with the time constant of  $\tau$  given in Table III.

### C. Reliability calculation of active switches

The two main factors affecting the lifetime of active devices are junction temperature and temperature swing of the device. Number of cycles to failure ( $N_f$ ) for an active switch like Diode and IGBT is related to the minimum junction temperature ( $T_{jm}$ ) and temperature swing ( $\Delta T_j$ ) as (3)[16] as:

$$N_f = A \cdot \Delta T_j^\alpha \cdot \exp\left(\frac{\beta}{T_{jm}}\right) \cdot \left(\frac{t_{on}}{1.5}\right)^{-0.3}, \quad (3)$$

$$0.1s \leq t_{on} \leq 60s$$

where  $A$ ,  $\alpha$  and  $\beta$  are the curve fitting parameters from the empirical tests reported in [16], and  $t_{on}$  being the thermal heating time in each cycle. In this paper,  $A = 9.34 \times 10E14$ ,  $\alpha = -4.416$  and  $\beta = 1290$ . The accumulated damage of the active switches ( $AD_s$ ) under different power cycling can be found as (4):

$$AD_s = \sum_{h=1}^H \frac{n_{cycle,h}}{N_{f,h}} \quad (4)$$

where  $n_{cycle,h}$  is the number of cycles for  $h^{th}$  power cycle and  $N_{f,h}$  is the number of cycles to failure with the same  $T_{jm}$  and  $\Delta T_j$  in  $h^{th}$  power cycle, which can be calculated by (3).  $H$  is

the total number of power cycles induced by the applied mission profile.

Dynamic thermal variables of each power cycle on the mission profile including  $t_{on}$ ,  $T_{jm}$  and  $\Delta T_j$  can be translated into static variables with the same degradation on the devices [17]. These values can be employed to estimate the lifetime of a device under the applied mission profile with constant parameters in the lifetime model provided in (3). In practice, the lifetime model and thermal stresses have stochastic behavior, and the uncertainty on these parameters should be considered in lifetime estimation [7]. Therefore, Monte-Carlo simulation can be employed to extract the failure density function and lifetime of each devices. Hence, the reliability function of each device can be found by fitting the data with the Weibull distribution. In the case that more than one IGBT/Diode are used, the overall IGBTs/Diodes reliability can be found by series reliability network model. The procedure of the reliability calculation for active switches is shown in Fig. 4 (b).

### D. Overall converter reliability

Since there are test results for electrolytic capacitors, the reliability of capacitors is obtained from real test data. However, for the active switches, lifetime is available only and hence Monte-Carlo simulation is employed to find the corresponding reliability function. In the studied converters, the whole converter will fail if one of the components, i.e., capacitor or diode or IGBT fails. Hence, as shown in Fig. 4 (c), the reliability of a converter ( $R_T$ ) can hence be found by series reliability network model as  $R_T = R_C \times R_Q \times R_D$ , where  $R_C$ ,  $R_Q$  and  $R_D$  are the reliability function of capacitors, IGBTs and Diodes respectively.

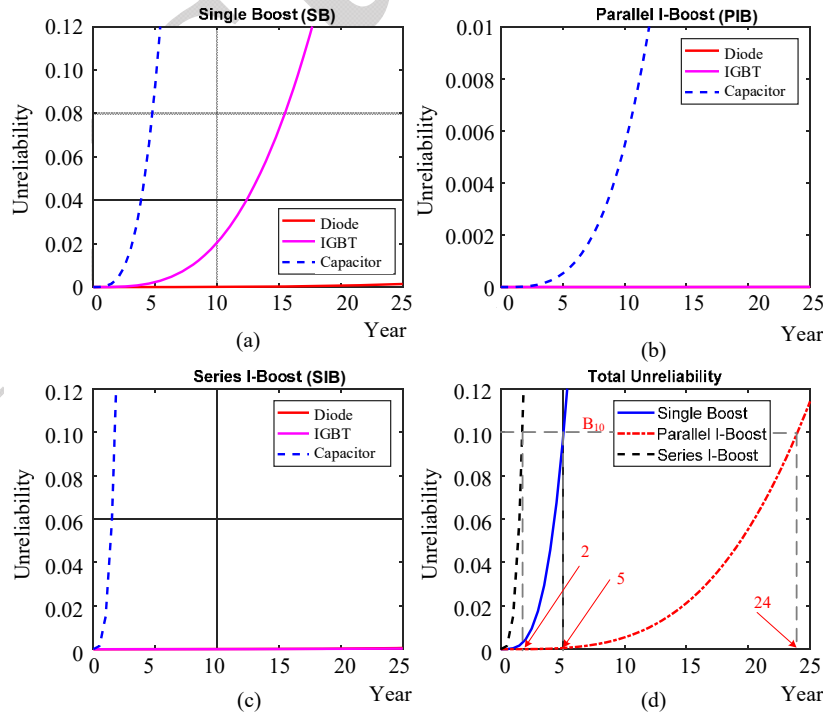


Fig. 5. Unreliability function of converters under the climate conditions in location A. Unreliability function of different components in (a) SB, (b) PIB, (c) SIB, and (d) total unreliability of each converter.

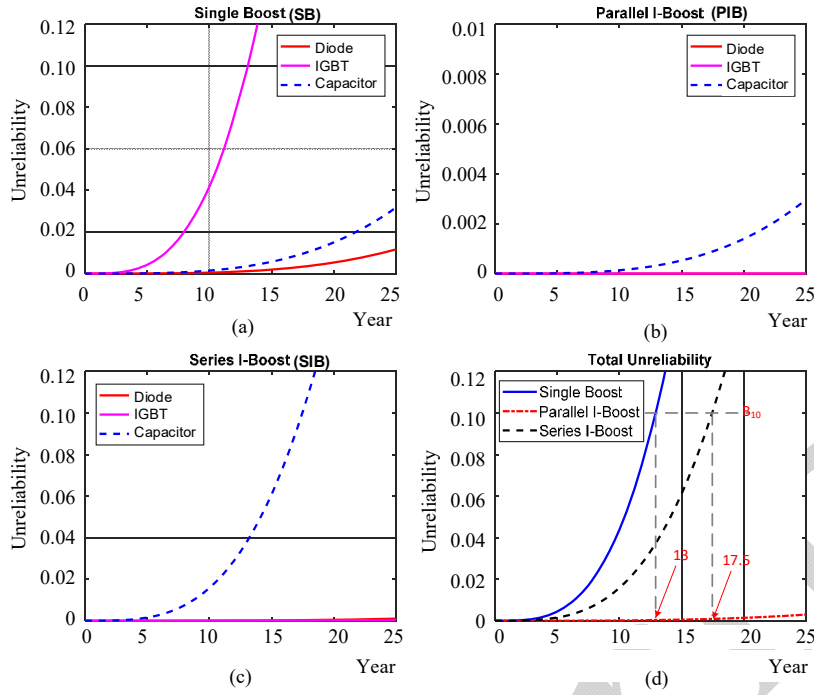


Fig. 6. Unreliability function of converters under climate condition in location B. Unreliability function of different components in (a) SB, (b) PIB, (c) SIB, and (d) total unreliability of each converter.

#### IV. RESULTS AND DISCUSSIONS

The reliabilities of the converters are estimated under the two mission profiles for locations A and B as shown in Fig. 2. The reliability of each components in SB, PIB and SIB is shown in Fig. 5 (a, b, c) for location A, and Fig. 6 (a, b, c) for location B. Furthermore, the total converter reliability is shown in Fig. 5 (d) and Fig. 6 (d) respectively for locations A and B. These results show the impact of mission profile and converter topology on the reliability of dc/dc energy conversion stage of PV converters. The obtained results are summarized as follows:

**Result 1:** As shown in Fig. 5 (a, b, c), the capacitor has the main contribution in the failure of all three types of converters for location A. However, for location B as shown in Fig. 6 (a), the IGBT has the highest effect on the reliability of SB converter, while, the reliability of the PIB and SIB is dominantly dependent on the capacitor bank as shown in Fig. 6 (b, c).

In order to further investigate the reliability of the SB converter, the annual accumulated damage on the IGBT, diode and capacitor bank under mission profiles A and B are reported in Fig. 7 (a). As shown in Fig. 7 (a), the capacitor bank has the highest damage under mission profile A, where the damage of the IGBT and diode is negligible. However, in location B, the capacitor damage is almost comparable with that of IGBT and diode. Following Fig. 2, the annual converted power by PV in location A is greater than location B. Consequently, the loading of the SB capacitor bank under mission profile A is higher than mission profile B. Meanwhile, according to Fig. 7 (b), the mission profile A induces much power cycling (current

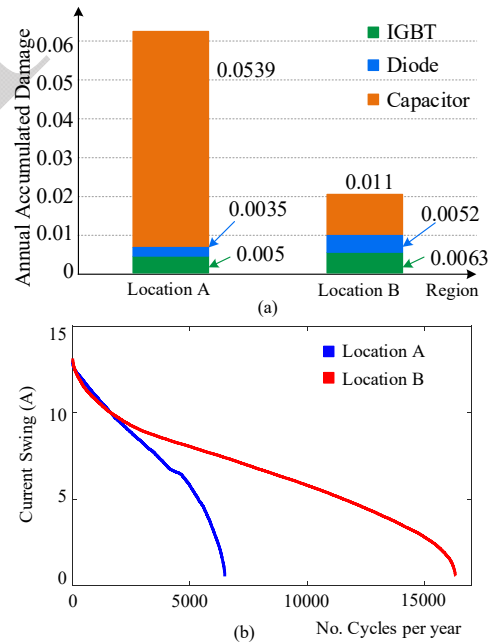


Fig. 7. SB converter damage analysis; (a) Annual accumulated damage on the components of converter and (b) converter power cycling (current swing) for both locations.

swing) on the converter, which is the mutual impact of solar irradiance and ambient temperature. Therefore, the IGBT and Diode have much stress and damage under mission profile B compared to the mission profile A. Considering the reliability estimation procedure, the reliability of the SB converter in location B depends on the active switches, where in location A, the capacitor bank has the dominant impact.

Furthermore, comparing the SIB and SB converters with the selected switching frequencies given in Table I, the thermal stress, and hence, the damage of the SIB's switches is small. Consequently, the contribution of active switches on the converter reliability is insignificant as shown in Fig. 5 (c) and Fig. 6 (c). Furthermore, the output capacitor bank of SIB consists of two series connected capacitor banks with five parallel-connected  $220 \mu F$  capacitors in order to obtain 0.5 % voltage ripple and withstand the ripple currents. Comparing to the capacitor bank of SB converter with four parallel-connected  $120 \mu F$  capacitors, the contribution of the capacitor bank in SIB is much higher than that of SB converter as it employs higher number of the capacitors as well as the higher thermal resistance as mentioned in Table III. Therefore, even though the loading of capacitor banks are lower under mission profile B, it still has the main contribution on the reliability of SIB converter under both mission profiles.

In the case of PIB converter, considering the selected switches for each topology (see Table I), the conduction and switching losses of SB is more than two times of PIB, while the rated current of PIB's switches is almost half of SB's. Consequently, the junction temperature rise in PIB is much smaller than that of in SB at the corresponding rated values. Hence, the contribution of the active switches on the converter reliability under both mission profiles is insignificant as shown in Fig. 5 (b) and Fig. 6 (b). The capacitor bank still has the dominant impact on the reliability of the PIB.

**Result 2:** Comparing the unreliability of the converters shown in Fig. 5 (d) with Fig. 6 (d), the PIB is the most reliable converter under both mission profiles. From Fig. 5 (b) and Fig. 6 (b), the output capacitor is the dominant component affecting the PIB reliability. Furthermore, applying the  $180^\circ$  phase shift between the carrier signals in PIB significantly reduces the ripple current of the output capacitor, and consequently, improves the reliability of the converter.

**Result 3:** From Fig. 5 (d) and Fig. 6 (d), in location A, the SB converter has better lifetime than the SIB. However, for location B, the SIB converter is more suitable than the SB converter. This is due to the impact of topology, which is related to the switching frequency affecting the reliability of active switches as well as the output voltage ripple and current affecting the design of capacitors. The influence of both factors are discussed in Result 1 highlighting the applicability of suitable topologies for different locations.

**Result 4:** Furthermore, comparing Fig. 5 (d) with Fig. 6 (d), the converters with a design based on the rated power of PV system may not have the same lifetime for different locations. Following Fig. 2, location A has greater ambient temperature along with higher annual converted energy. Thereby, the converter loading, and hence, the thermal stress on the components are not equal. For instance, following Fig. 7 (a), the accumulated damage on the components of the SB significantly depends on the mission

profile. Notably, using the SB converter in location A gives a  $B_{10}$  lifetime of 5 years as shown in Fig. 5 (d), while in location B, it has  $B_{10}$  lifetime of 13 years as shown in Fig. 6 (d).

## V. CONCLUSION

This paper studies the impact of mission profile and converter topology on the reliability of the dc/dc energy conversion stage in PV applications. Three dc/dc converter topologies with the same rated power, input current and output voltage ripples are considered, and the reliability of the converters are obtained with the climate data of two different locations. The contribution of active switches and capacitors on the reliability of converters is demonstrated where in some cases capacitors have more contribution and in some cases the IGBTs have more impact on the converter reliability. This study shows that the climate condition and topology are the two main factors affecting the lifetime of the converters, and hence, they should be considered during design procedure. For instance, following this study, Parallel Interleaved Boost (PIB) has the highest lifetime for the both mentioned locations. Moreover, Series Interleaved Boost (SIB) has the lowest lifetime if it is used in location A, while the Single Boost (SB) has the lowest reliability for location B.

## REFERENCES

- [1] S. M. Shinde, K. D. Patil, S. S. Khairnar, and W. Z. Gandhare, "The Role of Power Electronics in Renewable Energy Systems Research and Development," in *Proc. Second International Conference on Emerging Trends in Engineering & Technology*, 2009, pp. 726–730.
- [2] F. Blaabjerg and Ke Ma, "Future on Power Electronics for Wind Turbine Systems," *IEEE J. Emerg. Sel. Top. Power Electron.*, vol. 1, no. 3, pp. 139–152, Sep. 2013.
- [3] D. Boroyevich, I. Cvetkovic, R. Burgos, and D. Dong, "Intergrid: A Future Electronic Energy Network?," *IEEE J. Emerg. Sel. Top. Power Electron.*, vol. 1, no. 3, pp. 127–138, 2013.
- [4] S. Peyghami, P. Davari, and F. Blaabjerg, "System-Level Lifetime-Oriented Power Sharing Control of Paralleled DC/DC Converters," in *Proc. IEEE APEC*, 2018, pp. 1890–1895.
- [5] H. Wang, K. Ma, and F. Blaabjerg, "Design for Reliability of Power Electronic Systems," in *Proc. IEEE IECON*, 2012, pp. 33–44.
- [6] D. Zhou, H. Wang, and F. Blaabjerg, "Mission Profile Based System-Level Reliability Analysis of DC/DC Converters for a Backup Power Application," *IEEE Trans. Power Electron.*, p. Early Access, 2018.
- [7] P. D. Reigosa, H. Wang, Y. Yang, and F. Blaabjerg, "Prediction of Bond Wire Fatigue of IGBTs in a PV Inverter under a Long-Term Operation," *IEEE Trans. Power Electron.*, vol. 31, no. 10, pp. 3052–3059, Mar. 2016.
- [8] Y. Yang, A. Sangwongwanich, and F. Blaabjerg, "Design for Reliability of Power Electronics for Grid-Connected Photovoltaic Systems," *CPSS Trans. Power Electron. Appl.*, vol. 1, no. 1, pp. 92–103, Dec. 2016.
- [9] A. Khosroshahi, M. Abapour, and M. Sabahi, "Reliability Evaluation of Conventional and Interleaved DC–DC



- Boost Converters,” *IEEE Trans. Power Electron.*, vol. 30, no. 10, pp. 5821–5828, Oct. 2015.
- [10] H. Calleja, F. Chan, and I. Uribe, “Reliability-Oriented Assessment of a DC/DC Converter for Photovoltaic Applications,” in *Proc. IEEE PESC*, 2007, pp. 1522–1527.
- [11] F. H. Aghdam and M. Abapour, “Reliability and Cost Analysis of Multistage Boost Converters Connected to PV Panels,” *IEEE J. Photovoltaics*, vol. 6, no. 4, pp. 981–989, Jul. 2016.
- [12] S. V. Dhople, A. Davoudi, A. D. Domínguez-García, and P. L. Chapman, “A Unified Approach to Reliability Assessment of Multiphase DC–DC Converters in Photovoltaic Energy Conversion Systems,” *IEEE Trans. Power Electron.*, vol. 27, no. 2, pp. 739–751, Feb. 2012.
- [13] Department of Defense of the USA, “Reliability Prediction of Electronic Equipment,” *Mil. Handb. MIL-HDBK-217F*, p. 205, 1991.
- [14] EN 50530:2010 + A1:2013, “Overall Efficiency of Grid Connected Photovoltaic Inverters,” 2013.
- [15] A. Albertsen, “Electrolytic Capacitor Lifetime Estimation,” *JIANGHAI Eur. GmbH*, pp. 1–13, 2010.
- [16] R. Bayerer, T. Herrmann, T. Licht, J. Lutz, and M. Feller, “Model for Power Cycling Lifetime of IGBT Modules - Various Factors Influencing Lifetime,” in *5th International Conference on Integrated Power Systems (CIPS)*, 2008, pp. 1–6.
- [17] J. McPherson, “*Reliability Physics and Engineering*,” 2nd ed. Switzerland: Springer Int., 2013.